PROCEEDINGS OF SCIENCE

Measurement of Feynman-x Spectra of Photons and Neutrons in the Very Forward Direction in DIS at HERA

J. Olsson* **(on behalf of the H1 Collaboration)**
DESY, Hamburg, Germany
E-mail: jan.olsson@desy.de

H1 ep scattering data taken at HERA in the years 2006-7 are used to measure the production of very forward directed photons and neutrons. Normalised cross sections are given as a function of Feynman-x and of W, the centre-of-mass energy of the virtual photon-proton system. The phase space covered is defined by the ranges $6 < Q^2 < 100$ GeV^2, $0.05 < y < 0.6$, $70 < W < 245$ GeV and $\eta > 7.9$, where Q^2 is the photon virtuality, y the inelasticity and η the pseudorapidity in the laboratory frame. The integrated luminosity is 131 pb^{-1}. Comparisons to the data are made with the predictions of several deep-inelastic scattering models, as well as with the predictions of a number of models used in cosmic ray physics for the simulation of hadronic interactions in the Earth atmosphere. The hypothesis of Feynman Scaling is tested, by studying the W-dependence of the cross sections differential in Feynman-x. This is the first direct experimental test of Feynman Scaling for photon and neutron production in the very forward direction.

XXII. International Workshop on Deep-Inelastic Scattering and Related Subjects - DIS2014,
28 April - 2 May 2014
Warsaw, Poland

*Speaker.

1. Introduction

At the ep collider HERA the study of forward production of baryons (protons and neutrons) and photons has long been a subject of interest [1]. The term "forward" here implies that the produced particles have small polar angles with respect to the proton beam direction and carry a large fraction of the incoming proton longitudinal momentum. The early studies of forward baryon production at HERA [2, 3] showed that models of deep-inelastic scattering (DIS) are able to reproduce the data, but only if several production mechanisms are taken into account: string fragmentation, pion exchange, proton diffractive dissociation and elastic ep scattering. While the production mechanism for forward photons is almost solely the proton fragmentation, through the decay of neutral mesons from the fragmentation process, forward neutrons can also be produced in the colour singlet (pion) exchange process (Figure 1a,b). The fact that different production mechanisms have to be invoked for the simultaneous measurement of forward photons and neutrons is a challenge for the Monte Carlo (MC) simulation models. While it was found in a previous H1 analysis [3] that the forward neutron production can be well described as a sum of fragmentation and pion exchange processes, the forward photon production was in contrast found to be overestimated in the models, by large amounts (50-70%) [4]. Thus, very forward neutron and photon production offers a test of commonly used simulation models in an extreme corner of phase space.

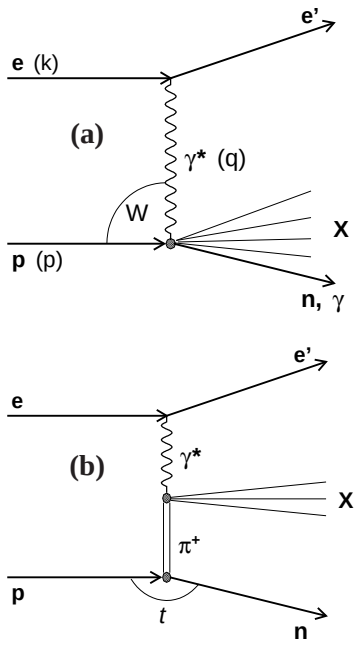

Figure 1: Diagrams for Neutron and Photon Production

Interest in the forward production of baryons and photons also arises in Cosmic Ray (CR) physics [5]. To estimate the energy of air shower initiating cosmic rays, extensive simulation of the hadronic interactions in the Earth atmosphere is needed, and several programs have been developed over the years for this purpose. For the calibration and tuning of such programs, forward scattering data obtained under controlled conditions, i.e. in high energy accelerator experiments, are needed. Such data are however surprisingly scarce. Thus, another motivation for the present study, and the presentation of the data in terms of the Feynman-x variable, was requests from the CR community.

The data presented here were taken in the last years of HERA operation, 2006-7, and consist of 131 pb^{-1}, taken at the ep centre-of-mass (CM) energy $\sqrt{s} = 319$ GeV. Neutrons and photons are detected in the H1 Forward Neutron Calorimeter (FNC) and to distinguish photons and neutrons the FNC Preshower is used. The latter is an electromagnetic calorimeter situated in front of the FNC Main Calorimeter. The aperture of the FNC, as given by the HERA beam optics elements, is limited to 0.75 mrad ($\eta > 7.9$, where η is the pseudorapidity in the laboratory frame).

The present analysis was recently published [6], as a continuation of the earlier analyses of forward neutrons [3] and forward photons [4]; thus, for details more than can be given here, please see these papers.

NC DIS Selection	
$6 < Q^2 < 100$ GeV^2	
$0.05 < y < 0.6$	
$70 < W < 245$ GeV	
Forward photons	**Forward neutrons**
$\eta > 7.9$	$\eta > 7.9$
$0.1 < x_F < 0.7$	$0.1 < x_F < 0.94$
$0 < p_T^* < 0.4$ GeV	$0 < p_T^* < 0.6$ GeV
W **ranges for cross sections** $\frac{1}{\sigma_{DIS}} \frac{\mathrm{d}\sigma}{\mathrm{d}x_F}$	
$70 < W < 130$ GeV	
$130 < W < 190$ GeV	
$190 < W < 245$ GeV	

Table 1: Definition of the kinematic phase space of the measurements.

2. Data sample

The data selection cuts are summarised in Table 1. Note that the ranges of x_F, the Feynman-x variable, differ for neutrons and photons. x_F is defined as $x_F = 2p_{||}^*/W$, where $p_{||}^*$ is the longitudinal momentum of the particle in the virtual photon-proton CM frame, with respect to the direction of the beam proton[1]. The lower value of the upper bound on x_F for photons is motivated by the wish to define the cross section for single photons; as seen in MC simulations, at larger x_F values electromagnetic clusters in the FNC Preshower are mainly caused by unresolved double photons (from π° decays). The common lower bound $x_F = 0.1$ corresponds to lower values of about 92 GeV for the FNC cluster energies. The difference in upper bounds on the transverse momentum p_T^* is a consequence of the different upper bounds on x_F.

For the purpose of the test of the Feynman Scaling hypothesis, the W range is divided into three intervals. For the results presentation, the cross sections are normalised to the total DIS cross section.

The total sample, after all cuts, consists of $\sim 230,000$ neutron events and $\sim 83,000$ photon events.

3. MC Models

For the basic simulation of DIS events the leading order MC program DJANGOH [7] is used.

[1] In the kinematic range of this measurement the variable x_F is numerically almost equal to the longitudinal momentum fraction x_L used in previous publications. There, x_L was defined as $x_L = E_{n,\gamma}/E_p$, where E_p, E_n and E_γ are the energies of the proton beam, the forward neutron and the forward photon in the laboratory frame, respectively.

For higher order QCD effects DJANGOH is combined with either LEPTO [8] or ARIADNE [9]; the former program provides leading log parton showers and the latter uses the Colour Dipole Model (CDM). These combinations are here labelled "LEPTO" and "CDM". The pion exchange process is modelled with the program RAPGAP [10], with the option of exclusive scattering of the virtual (or real) photon on an exchanged pion; this simulation is here labelled "RAPGAP-π". The pion flux used is taken from [11]. All programs use HERACLES [12] for higher order electroweak processes, and hadronisation is made using JETSET [13].
As shown in [3], equally good descriptions of the forward neutron production are obtained with weighted combinations of either LEPTO + RAPGAP-π or CDM + RAPGAP-π; while pion exchange dominates at higher neutron energies, the lower energies are dominated by neutrons from proton fragmentation. Surprising is the big difference (factor 2) between the respective scale factors for LEPTO and CDM: either $0.7\times$LEPTO + $0.6\times$RAPGAP-π or $1.4\times$CDM + $0.6\times$RAPGAP-π. Thus, although CDM overestimates the forward photon production by $\sim 70\%$, it has to be scaled up by 1.4 in order to describe the forward neutron production.
Several models used for the simulation of cosmic ray air showers are also compared to the data: EPOS LHC [14], QGSJET 01 [15], QGSJET II-04 [16] and SIBYLL 2.1 [17]. These models have been developed over many years, and are based both on older (Regge theory, Gribov's Regge Calculus) and newer concepts, such as perturbative QCD. Central elements are mini-jets production and colour string fragmentation into hadrons.
All programs have been interfaced to the HERA ep scattering kinematics via the PHOJET [18] program. All program simulations used for the comparison with the data have been provided by the respective authors; no adjustment of internal parameters were made from the H1 side.

4. Results

4.1 The W-dependence of the cross sections

Figure 2 shows the W-dependence of the normalised cross sections, for photons (Figure 2a,b) and neutrons (Figure 2c,d). The cross sections are within uncertainties constant, at values of ~ 0.027 and ~ 0.083, respectively. As already mentioned, the MC DIS predictions of LEPTO and CDM for photons are much above the data (Figure 2a) and also the CR models predict substantially higher photon rates (Figure 2b); moreover, all MC models except CDM predict a slight W-dependence of the cross section. Also the neutron cross section shows a slight W-dependence in all MC predictions (except RAPGAP-π); good descriptions of the data are however obtained by weighted combinations of RAPGAP-π with either LEPTO or CDM. None of the CR models describe the neutron data, although EPOS LHC and QGSJET II-04 are closer than SIBYLL and QGSJET 01.

4.2 The x_F-dependence of the cross sections

The normalised cross sections differential in x_F are shown for photons in (Figure3a,b) and for neutrons in (Figure3c,d). Only the distributions in the W-interval $70-130$ GeV are given here, the

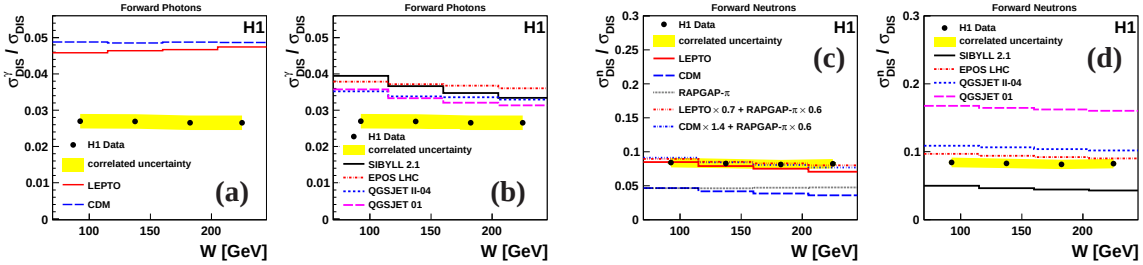

Figure 2: The fraction of DIS events with forward photons **(a, b)** and forward neutrons **(c,d)** as a function of W. Also shown **(a,c)** are the predictions of the LEPTO and CDM MC models. In **(c)**, the predictions of RAPGAP-π and the linear combinations of LEPTO and RAPGAP-π, as well as CDM and RAPGAP-π are shown. In **(b,d)** the CR model predictions are compared to the data.

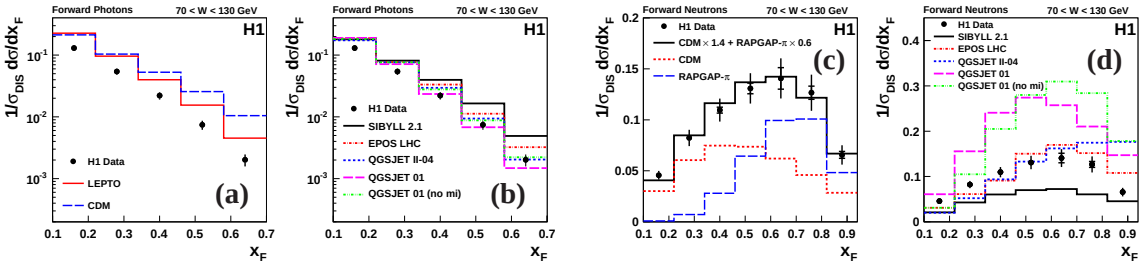

Figure 3: Normalised cross sections of forward photon **(a,b)** and neutron **(c,d)** production in DIS as a function of x_F in the W-interval $70-130$ GeV. Also shown **(a)** are the predictions of the LEPTO and CDM MC models. In **(c)**, the predictions of CDM, RAPGAP-π and the linear combination of CDM and RAPGAP-π are shown. In **(b,d)** the CR model predictions are compared to the data.

distributions in the two higher W-intervals are similar.

As in the W-dependence case, the MC DIS predictions for photons of LEPTO and CDM (Figure3a) lie 50-70% above the data. The x_F-dependence is rather well predicted by LEPTO; in contrast the CDM x_F-dependence is much too hard. The CR model predictions for photons (Figure3b) vary for the x_F-dependence, and are in general above the data for low values of x_F. In the neutron x_F-dependence the high values are dominated by the pion exchange, as simulated by RAPGAP-π (Figure3c), while the lower values correspond to the proton fragmentation, as given by CDM (or LEPTO, not shown). The CR models (Figure3d) vary greatly in the neutron x_F-dependence and again EPOS LHC and QGSJET II-04 are closer to the data than SIBYLL and QGSJET 01.

Since the CR models were concipated for hadronic interactions, a modified version of QGSJET 01, denoted "QGSJET 01 (no mi)" was also compared to the data; in this version the effects of multi-parton interactions are switched off, with the idea that this is more appropriate for the ep DIS environment. As seen (Figure3d), the description of the neutron x_F-data is not improved and instead becomes significantly harder at large values of x_F.

4.3 Test of Feynman Scaling

The measured cross sections, differential in W and x_F, offer the possibility of performing a direct experimental test of the Feynman Scaling hypothesis [19]. For this purpose the $d\sigma/dx_F$-distributions in the two higher W-intervals, 130-190 and 190-245 GeV, are divided with the cor-

responding $d\sigma/dx_F$-distributions in the lowest W-interval, 70-130 GeV. The resulting ratios, as a function of x_F, are shown for photons in Figures 4a-d and for neutrons in Figures 5a,b. Within errors the ratios are compatible with unity, i.e. the x_F-distributions stay practically unchanged with increasing W. This is the first direct experimental test of Feynman Scaling for forwardly produced neutrons and photons at HERA.

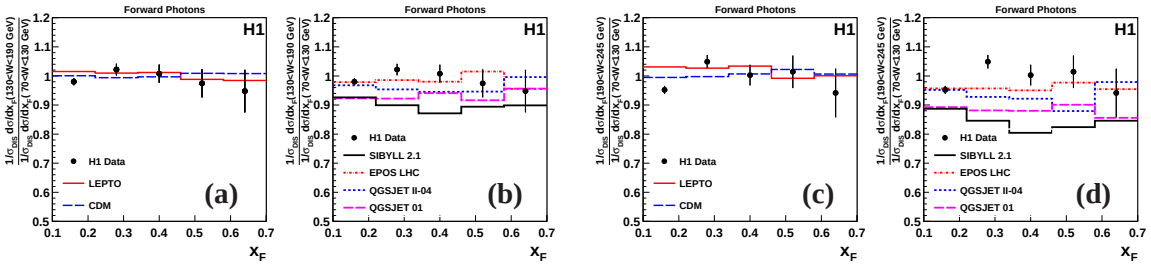

Figure 4: Ratios of normalised cross sections of forward photon production in DIS corresponding to two different W intervals, as a function of x_F: respectively the ratio of the cross section in the $130 < W < 190$ GeV **(a,b)** and $190 < W < 245$ GeV **(c,d)** interval to the cross section in the $70 < W < 130$ GeV interval. Predictions of the LEPTO and CDM MC models are shown in **(a,c)** and of the CR models in **(b,d)**.

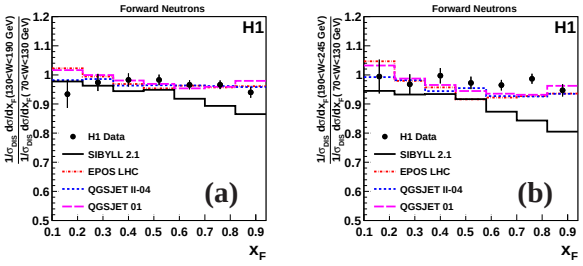

Figure 5: Ratios of normalised cross sections of forward neutron production in DIS corresponding to two different W intervals, as a function of x_F: respectively the ratio of the cross section in the $130 < W < 190$ GeV **(a)** and $190 < W < 245$ GeV **(b)** interval to the cross section in the $70 < W < 130$ GeV interval. Predictions of the CR models are also shown.

In previous analyses ([3, 4]) the neutron and photon data were shown to confirm the hypothesis of limiting fragmentation [20]. The hypotheses of limiting fragmentation and of Feynman scaling both stem from the same time, late 1969, and both hypotheses were put forward independently. They are based on the same simple fact, namely the Lorentz contraction of the beam projectile, and both hypotheses aim at finding regularities in multi-particle production at high energies. While the hypothesis of limiting fragmentation states that single particle momentum distributions at high energy are limited by functions solely dependent on transverse momentum and rapidity, Feynman scaling states independence of particle distributions at high energy when expressed as functions of transverse momentum and Feynman-x only. Since the variables rapidity and Feynman-x are related[2], the two hypotheses are equivalent. It is therefore not unexpected that the same neutron and photon data in the present direct experimental test confirm the hypothesis of Feynman scaling.

[2]The relation between x_F and rapidity y is $x_F = 2\mu/Wsinh(y)$, $\mu = \sqrt{p_t^2 + m^2}$.

5. Acknowledgement

Many thanks to all colleagues in H1, in particular to A.Bunyatyan and H.Zohrabyan, for providing the material in this report and for help given in its preparation. Warm thanks also to the Warsaw team for the excellent organisation and the pleasant atmosphere of the conference.

References

[1] R. Engel, Nucl. Phys. Proc. Suppl. **75A** (1999) 62 [astro-ph/9811225].

[2] C. Adloff *et al.* [H1 Collaboration], Eur. Phys. J. **C6** (1999) 587 [hep-ex/9811013];
S. Chekanov *et al.* [ZEUS Collaboration], Nucl. Phys. **B637** 3 (2002) 3 [hep-ex/0205076];
S. Chekanov *et al.* [ZEUS Collaboration], Nucl. Phys. **B776** (2007) 1 [hep-ex/0702028];
S. Chekanov *et al.* [ZEUS Collaboration], JHEP **06** (2009) 074 [arXiv:0812.2416].

[3] F. Aaron *et al.* [H1 Collaboration], Eur. Phys. J. **C68** (2010) 381 [arXiv:1001.0532].

[4] F. Aaron *et al.* [H1 Collaboration], Eur. Phys. J. **C71** (2011) 1771 [arXiv:1106.5944].

[5] A. Buniatyan *et al.*, *"Cosmic Rays, HERA and the LHC: Working group summary."* Proceedings of the Workshop on the Implications of HERA for LHC Physics, Geneva, Switzerland, 26-30 May 2008, p.566, DESY-PROC-2009-02 [arXiv:0903.3861].

[6] V. Andreev *et al.* [H1 Collaboration], DESY 14-035 [arXiv:1404.0201].

[7] K. Charchula, G. A. Schuler and H. Spiesberger, Comput. Phys. Commun. **81** (1994) 381.

[8] G. Ingelman, A. Edin and J. Rathsman, Comput. Phys. Commun. **101** (1997) 108 [hep-ph/9605286];
A. Edin, G. Ingelman and J. Rathsman, Phys. Lett. **B366** (1996) 371 [hep-ph/9508386].

[9] L. Lönnblad, Comput. Phys. Commun. **71** (1992) 15.

[10] H. Jung, Comp. Phys. Commun. **86** (1995) 147.

[11] H. Holtmann *et al.*, Phys. Lett. **B338** (1994) 363.

[12] A. Kwiatkowski, H. Spiesberger and H. J. Möhring, Comp. Phys. Commun. **69** (1992) 155.

[13] B. Andersson *et al.*, Phys. Rep. **97** (1983) 31; T. Sjöstrand, [hep-ph/9508391].

[14] K. Werner, F.-M. Liu and T. Pierog, Phys. Rev. **C74** (2006) 044902 [hep-ph/0506232];
T. Pierog *et al.*, DESY-13-125 [arXiv:1306.0121].

[15] N. N. Kalmykov and S. S. Ostapchenko, Phys. Atom. Nucl. **56** (1993) 346;
N. N. Kalmykov, S. S. Ostapchenko and A. I. Pavlov, Nucl. Phys. Proc. Suppl. **52B** (1997) 17.

[16] S. S. Ostapchenko, Phys. Rev. **D74** (2006) 014026 [hep-ph/0505259];
S. S. Ostapchenko, Phys. Rev. **D83** (2011) 014018 [arXiv:1010.1869].

[17] J. Engel *et al.*, Phys. Rev. **D46** (1992) 5013;
E.-J. Ahn *et al.*, Phys. Rev. **D80** (2009) 094003 [arXiv:0906.4113].

[18] R. Engel and J. Ranft, Phys. Rev. **D54** (1996) 4244 [hep-ph/9509373].

[19] R. P. Feynman, Phys. Rev. Lett. **23** (1969) 1415.

[20] J. Benecke *et al.*, Phys. Rev. **188** (1969) 2159;
T. T. Chou and C.-N. Yang, Phys. Rev. **D50** (1994) 590.